

Color Texture Restoration

Michal Haindl and Vojtěch Havlíček

Institute of Information Theory and Automation of the CAS

Prague, Czech Republic 182 08

Email: {haindl,havlicek}@utia.cas.cz

Abstract—Visual texture restoration strives not necessarily to recover the exact pixel-wise correspondence with some original unobservable texture but rather a texture which is visually indiscernible from the original one. This differs from the standard image restoration objective so it can consequently lead to different restoration techniques. A novel multispectral texture restoration method, capable to reduce simultaneously additive noise and to restore missing textural parts is presented. The restoration method is based on a descriptive, unusually complex, three-dimensional, spatial Gaussian mixture model. The model is inherently multispectral thus it does not suffer with the spectral quality compromises of the most alternative approaches.

I. INTRODUCTION

Physical imaging systems and a recording medium are imperfect and thus a recorded image represents a degraded version of the original scene. Similarly an image is usually further corrupted during its processing, transmission or storage. The image restoration task is to recover an unobservable image given the observed corrupted image with respect to some statistical criterion. Image restoration is the busy research area for already several decades and numerous restoration algorithms have been proposed [1], [2], [3], [4]. However, this ill-defined task is application dependent and far from being solved.

Visual texture typically represents a surface material appearance. Although, there is no mathematically rigorous definition of texture, textures share some common determining properties [5] such as homogeneity, scale dependency, etc.

Texture restoration slightly differs from the general image restoration in its ultimate goal, which is to recover the ideal unobservable original image. Texture restoration aim is not to recover the pixel-wise correspondence with such an original unobservable texture but rather a texture which is visually indiscernible from the original one. There are significantly fewer methods [6], [7], [8], [9], [10], [11], [12] focused on visual texture restoration and the majority of the model based techniques are restricted to gray-scale [8], [12] or even binary textures [11]. Some methods are restricted to noise restoration [9], [12] only. In-painting techniques cannot reduce noise and inevitably introduces more or less visible artifacts on restored scratch areas due to compromised patch replacement, e.g., [10].

The presented contribution is the high quality visual texture restoration method based on a non-trivial inherently multispectral spatial 3D Gaussian mixture model (3DGM), which has the noise restoration as well as the scratch removal capability.

II. SPATIAL 3D GAUSSIAN MIXTURE MODEL

A homogeneous static texture image Y is assumed to be defined on a finite rectangular $N_1 \times N_2 \times d$ lattice I , $r = (r_1, r_2, r_3) \in I$ denotes a pixel multiindex with the row, columns and spectral indices, respectively. Let us suppose that Y represents a realization of a random vector with a probability distribution $P(Y)$. The statistical properties of interior pixels of the moving window on Y are translation invariant due to assumed textural homogeneity. They can be represented by a joint probability distribution and the properties of the texture can be fully characterized by statistical dependencies on a sub-field, i. e., by a marginal probability distribution of spectral levels on pixels within the scope of a window centered around the location r and specified by the index set:

$$I_r = \{r + s : |r_1 - s_1| \leq \alpha \wedge |r_2 - s_2| \leq \beta\} \subset I .$$

The index set I_r depends on a modeled visual data and can have any other than this rectangular shape. $Y_{\{r\}}$ denotes the corresponding matrix containing all Y_s in some fixed order arrangement such that $s \in I_r$, $Y_{\{r\}} = [Y_s \ \forall s \in I_r]$, $Y_{\{r\}} \subset Y$, $\eta = \text{cardinality}\{I_r\}$ and $P(Y_{\{r\}})$ is the corresponding marginal distribution of $P(Y)$.

A. 3D Gaussian Mixture

If we assume the joint probability distribution $P(Y_{\{r\}})$, in the form of a normal mixture

$$\begin{aligned} P(Y_{\{r\}}) &= \sum_{m \in \mathcal{M}} p(m) P(Y_{\{r\}} | \mu_m, \Sigma_m) \quad Y_{\{r\}} \subset Y , \\ &= \sum_{m \in \mathcal{M}} p(m) \prod_{s \in I_r} p_s(Y_s | \mu_{m,s}, \Sigma_{m,s}) \end{aligned} \quad (1)$$

where $Y_{\{r\}} \in \mathbb{R}^{d \times \eta}$ is $d \times \eta$ matrix, μ_m is $d \times \eta$ mean matrix, Σ_m is $d \times d \times \eta$ a covariance tensor, and $p(m)$ are probability weights and the mixture components are defined as products of multivariate Gaussian densities

$$P(Y_{\{r\}} | \mu_m, \Sigma_m) = \prod_{s \in I_{\{r\}}} p_s(Y_s | \mu_{m,s}, \Sigma_{m,s}) , \quad (2)$$

$$\begin{aligned} p_s(Y_s | \mu_{m,s}, \Sigma_{m,s}) &= \frac{1}{(2\pi)^{\frac{d}{2}} |\Sigma_{m,s}|^{\frac{1}{2}}} \\ &\exp \left\{ -\frac{1}{2} (Y_r - \mu_{m,s})^T \Sigma_{m,s}^{-1} (Y_r - \mu_{m,s}) \right\} , \end{aligned} \quad (3)$$

i. e., the components are multivariate Gaussian densities with covariance matrices (7).

The underlying structural model of conditional independence is estimated from a data set \mathcal{S} obtained by the step-wise shifting of the contextual window I_r within the original texture image, i. e., for each location r one realization of $Y_{\{r\}}$.

$$\mathcal{S} = \{Y_{\{r\}} \mid \forall r \in I, I_r \subset I\} \quad Y_{\{r\}} \in \mathbb{R}^{d \times \eta} . \quad (4)$$

1) *Parameter estimation*: The unknown parameters of the approximating mixture can be estimated using the iterative EM algorithm [13]. In order to estimate the unknown distributions $p_s(\cdot | m)$ and the component weights $p(m)$ we maximize the likelihood function corresponding to the training set (4):

$$L = \frac{1}{|\mathcal{S}|} \sum_{Y_{\{r\}} \in \mathcal{S}} \log \left[\sum_{m \in \mathcal{M}} P(Y_{\{r\}} | \mu_m, \Sigma_m) p(m) \right] .$$

The likelihood is maximized using the iterative EM algorithm (with non-diagonal covariance matrices):

E:

$$q^{(t)}(m | Y_{\{r\}}) = \frac{\tilde{P}^{(t)}(Y_{\{r\}} | \mu_m, \Sigma_m) p^{(t)}(m)}{\sum_{j \in \mathcal{M}} \tilde{P}^{(t)}(Y_{\{r\}} | \mu_j, \Sigma_j) p^{(t)}(j)} ,$$

M:

$$p^{(t+1)}(m) = \frac{1}{|\mathcal{S}|} \sum_{Y_{\{r\}} \in \mathcal{S}} q^{(t)}(m | Y_{\{r\}}) , \quad (5)$$

$$\mu_{m,s}^{(t+1)} = \frac{1}{\sum_{Y_{\{r\}} \in \mathcal{S}} q^{(t)}(m | Y_{\{r\}})} \sum_{Y_{\{r\}} \in \mathcal{S}} Y_s q^{(t)}(m | Y_{\{r\}}) . \quad (6)$$

The $M\eta$ covariance matrices are:

$$\begin{aligned} \Sigma_{m,s}^{(t+1)} &= \frac{\sum_{Y_{\{r\}} \in \mathcal{S}, Y_s \in Y_{\{r\}}} q^{(t)}(m | Y_{\{r\}})}{\sum_{Y_r \in \mathcal{S}} q^{(t)}(m | Y_{\{r\}})} \\ &\quad (Y_s - \mu_{m,s}^{(t+1)})(Y_s - \mu_{m,s}^{(t+1)})^T \\ &= \frac{\sum_{Y_{\{r\}} \in \mathcal{S}, Y_s \in Y_{\{r\}}} q^{(t)}(m | Y_{\{r\}}) Y_s Y_s^T}{\sum_{Y_r \in \mathcal{S}} q^{(t)}(m | Y_{\{r\}})} \\ &\quad - \frac{p^{(t+1)}(m) |\mathcal{S}| \mu_{m,s}^{(t+1)} \left(\mu_{m,s}^{(t+1)} \right)^T}{\sum_{Y_r \in \mathcal{S}} q^{(t)}(m | Y_{\{r\}})} . \quad (7) \end{aligned}$$

The iteration process is stopped when the criterion increments are sufficiently small. The EM algorithm iteration scheme has the monotonic property: $L^{(t+1)} \geq L^{(t)}$, $t = 0, 1, 2, \dots$ which implies the convergence of the sequence $\{L^{(t)}\}_0^\infty$ to a stationary point of the EM algorithm (local maximum or a saddle point of L).

B. Texture Synthesis

The advantage of a mixture model is its simple synthesis based on the marginals:

$$p_{n|\rho}(Y_n | Y_{\{\rho\}}) = \sum_{m=1}^M W_m(Y_{\{\rho\}}) p_n(Y_n | m) , \quad (8)$$

where $W_m(Y_{\{\rho\}})$ are the a posteriori component weights corresponding to the given submatrix $Y_{\{\rho\}} \subset Y_{\{r\}}$:

$$\begin{aligned} W_m(Y_{\{\rho\}}) &= \frac{p(m) P_\rho(Y_{\{\rho\}} | m)}{\sum_{j=1}^M p(j) P_\rho(Y_{\{\rho\}} | j)} , \quad (9) \\ P_\rho(Y_{\{\rho\}} | m) &= \prod_{n \in \rho} p_n(Y_n | m) . \end{aligned}$$

The unknown multivariate vector-levels Y_n can be synthesized by random sampling from the conditional density (8) or the mixture RF can be approximated using the GMM mixture prediction.

1) *Prediction-Based Synthesis*: There are several alternatives for the 3DGMM model synthesis. The proposed method uses the 3DGMM model approximation by computing the conditional GMM expectation:

$$\begin{aligned} E\{Y_n\} &= \int Y_n p_{n|\rho}(Y_n | Y_{\{\rho\}}) dY_n \\ &= \sum_{j=1}^M W_j(Y_{\{\rho\}}) \mu_{jn} . \quad (10) \end{aligned}$$

This is a fast non-iterative alternative for a GMM model synthesis.

III. EXPERIMENTAL RESULTS

The proposed method is compared with an alternative, high-quality descriptive model-based restoration method [14] which can also restore additive noise as well as missing textural parts [15]. The performance of the tested methods is compared on artificially degraded textural images (so that the unobservable data are known) using the criterion of the mean absolute difference between undegraded and restored pixel values:

$$MAD = \frac{1}{n_1 n_2 d} \sum_{r_1=1}^{n_1} \sum_{r_2=1}^{n_2} \sum_{r_3=1}^d |Y_r - \hat{Y}_r| , \quad (11)$$

where $d = 3$ for color static textures (but d can be easily larger for hyperspectral textures), $n_1 = N_1$, $n_2 = N_2$ for additive noise restoration and $n_1 n_2$ is the number of missing pixels for the scratch restoration task. This criterion is not ideal because our texture restoration goal is not to recover the pixel-wise version of the original texture, but we accept any other original texture realisation which would be visually indiscernible from the original unobservable texture. Unfortunately, there is no any other reliable texture quality criterion as it was demonstrated in recent paper [16].

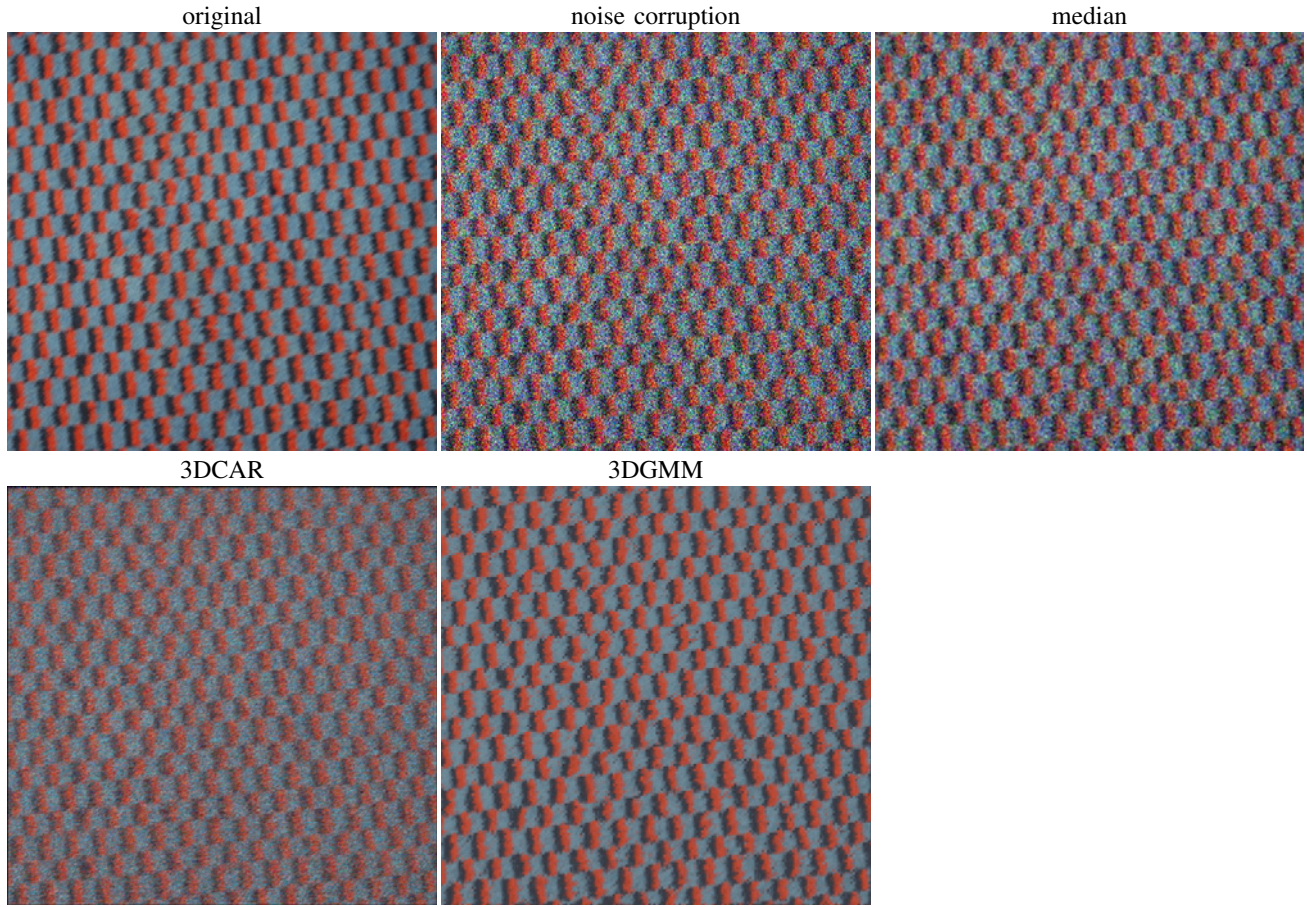


Fig. 1. Additive noise restoration results for the carpet texture.

The presented model has time consuming parameter estimation part compared with the fast analytic 3DCAR (Section III-A) alternative. The 3DGMM model has large set of parameters to be iteratively learned, which is the most time and computer memory demanding part of the method. The 3DGMM model has more parameters to be learned than the 3DCAR model and thus it requires also larger learning set ($|S|$). The analytical part of the EM algorithm can be speed up by K-means based components initialization. The model synthesis is not iterative and thus relatively fast. Another difference is that the 3DGMM model is global, while 3DCAR model restores textures locally. This is a disadvantage in strictly homogeneous textures where the global model uses better learned parameters, but it may be advantageous for slowly changing textures. The efficiency of the 3DCAR model is at the cost of possible artifacts due to model causality, while the presented model is non-causal and also multimodal.

A. Spatial CAR Model Based Texture Restoration

A spatial multispectral causal simultaneous autoregressive model based restoration was introduced [17] and [14]. Texture scratch removal can be performed using a modification of the same model (see details of the monospectral version of the scratch removal method in [15]).

The 3D causal simultaneous autoregressive model

(3DCAR) is the wide-sense Markov model which can be written in the following regression equation form:

$$\tilde{Y}_r = \sum_{s \in I_r^c} A_s \tilde{Y}_{r-s} + e_r \quad \forall r \in I \quad (12)$$

where A_s are matrices (13) and the zero mean white Gaussian noise vector e_r has uncorrelated components with data indexed from I_r^c but noise vector components can be mutually correlated with a constant covariance matrix Σ . $I_r^c \subset I$ is a causal or unilateral neighbourhood of pixel r , i.e.

$$I_r^c \subset I^C = \{s : 1 \leq s_1 \leq r_1, 1 \leq s_2 \leq r_2, s \neq r\} .$$

$$A_{s_1, s_2} = \begin{pmatrix} a_{1,1}^{s_1, s_2} & \dots & a_{1,d}^{s_1, s_2} \\ \vdots & \ddots & \vdots \\ a_{d,1}^{s_1, s_2} & \dots & a_{d,d}^{s_1, s_2} \end{pmatrix} \quad (13)$$

are $d \times d$ parameter matrices.

The model can be expressed in the matrix form

$$Y_r = \gamma X_r + e_r ,$$

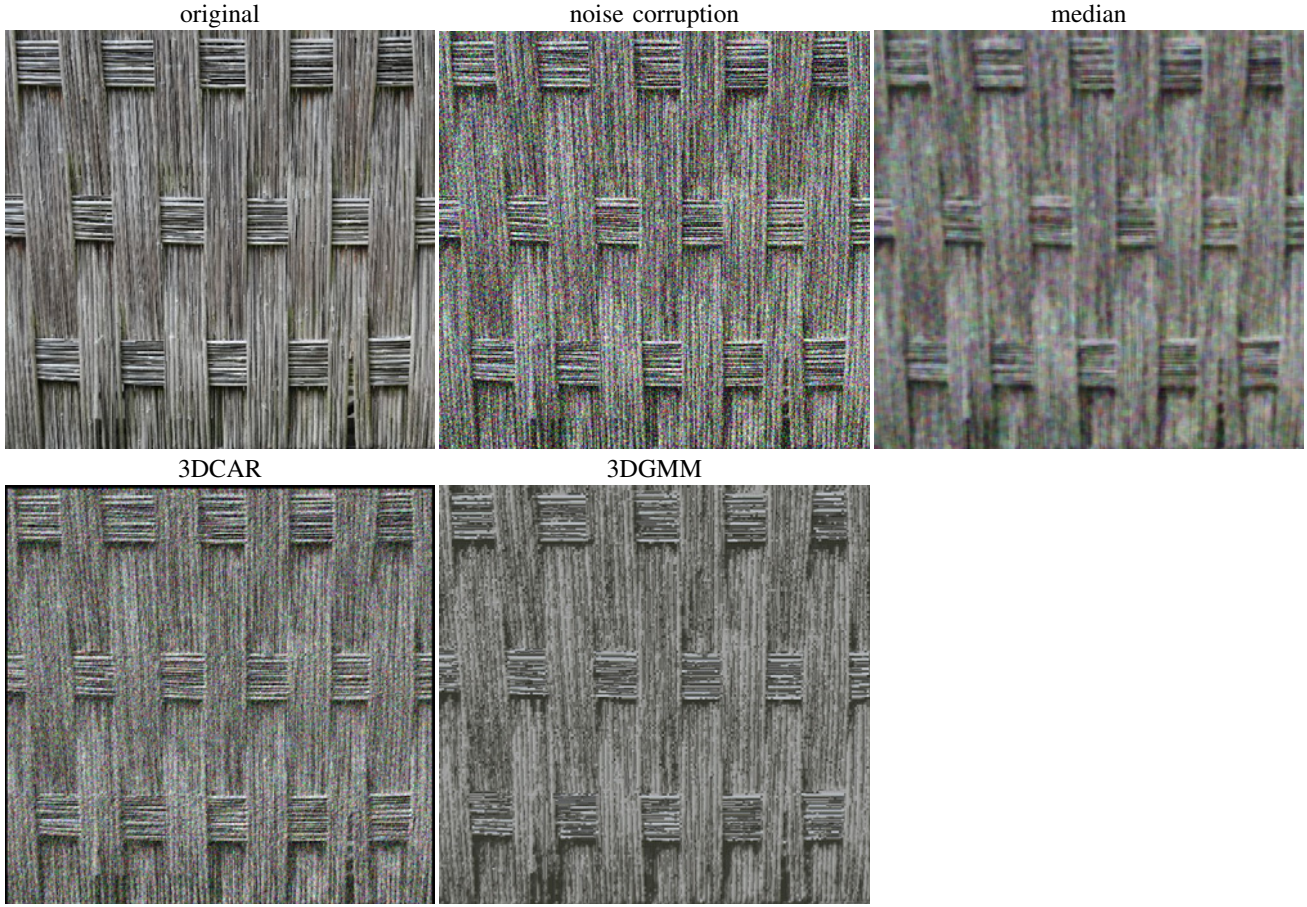


Fig. 2. Additive noise restoration results for the matting texture.

where

$$X_r = [\tilde{Y}_{r-s}^T : \forall s \in I_r^c] , \quad (14)$$

X_r is a $d\zeta \times 1$ vector, $\zeta = \text{cardinality}(I_r^c)$ and γ

$$\gamma = [A_1, \dots, A_\zeta] \quad (15)$$

is a $d \times d\zeta$ parameter matrix.

Additive noise is restored using (16). Pixels with steep step discontinuities are left unrestored to avoid excessive blurring, i.e.,

$$\hat{Y}_r = \begin{cases} E\{Y_r | Y^{(r-1)}\} & \text{if (17)} \\ Y_r & \text{otherwise} \end{cases} , \quad (16)$$

$$|E\{Y_r\} - Y_r| < \frac{1}{n_s} \sum_s |E\{Y_{r-s}\} - Y_{r-s}| , \quad (17)$$

where n_s is a selected adaptive threshold memory and $Y^{(r-1)}$ is the past process history of the model. Scratches are restored using the conditional predictor

$$\hat{Y}_r = E\{Y_r | Y^{(r-1)}\} . \quad (18)$$

The 3DCAR model is directional and thus it is advantageous to restore larger scratches using the nearest directional predictor (18) from the last completely known data.

B. Additive Noise Removal

Figs. 1, 2 demonstrate two typical performance examples of additive noise texture restoration. The original textures were corrupted with additive Gaussian noise $\mathcal{N}(0; 70)$ independently for all spectral bands (the upper row middle image in both Figs.). Textures were restored using either the median filter, 3DCAR model, or the proposed method. The corresponding MAD criterion numerical values are listed in Tab. I. The 3×3 , 5×5 , 7×7 median filters were tested and the best performing filter using the MAD criterion is listed in Tab. I and illustrated in Figs. 1, 2.

Tab. I demonstrates the best noise removal performance of our method and Fig. 1 illustrates the advantage of the presented global model over the locally restored texture using the 3DCAR method which slightly compromises the spectral quality of the restored texture.

Texture	Method	MAD
carpet	noise	51,75
carpet	median	16.85
carpet	3DCAR	21.82
carpet	3DGMM	13.12
matting	noise	51,34
matting	median	27.17
matting	3DCAR	30.84
matting	3DGMM	23.33

TABLE I. NOISE RESTORATION RESULTS ON THE CARPET AND MATTING TEXTURES.

C. Scratch Removal

Fig. 3 demonstrates scratch removal capability of the presented method in comparison with the 3DCAR method [15] which is also based on a spatial descriptive Markovian model. Although the 3DCAR method uses local adaptive prediction and performs well on purely stochastic textures, it is outperformed by the presented method on regular or near-regular textures and if there is large patch to be reconstructed. This visual observation is also confirmed numerically in Tab. II which is computed from the presented images in Fig. 3. Clearly visible deficiencies can be observed in the area of large removed texture rectangle.

Texture	Method	MAD
carpet	3DCAR	13,66
carpet	3DGMM	10,36
cobra	3DCAR	21,06
cobra	3DGMM	16,00
tiles	3DCAR	28,78
tiles	3DGMM	25,60

TABLE II. SCRATCH RESTORATION RESULTS ON THE CARPET, COBRA SKIN, AND TILES TEXTURES.

IV. CONCLUSIONS

The proposed color texture reconstruction method is capable to simultaneously reduce additive noise and restore missing textural parts. It produces high quality results especially of regular or near-regular color textures where it outperforms the alternative method based on Markovian descriptive model or median filter using the mean absolute difference between undegraded and restored pixel values criterion as well as visual observation. The presented model has time consuming parameter estimation part and requires larger learning set than the alternative simpler 3DCAR method. The model synthesis is not iterative and thus relatively fast.

The method can be also easily generalized for hyperspectral or bidirectional texture function (BTF) textures.

ACKNOWLEDGMENTS

This research was supported by by the Czech Science Foundation project GAČR 14-10911S.

REFERENCES

[1] H. C. Andrews and B. Hunt, *Digital Image Restoration*. Englewood Cliffs: Prentice-Hall, 1977. 1

[2] S. Geman and D. Geman, "Stochastic relaxation, gibbs distributions and bayesian restoration of images," *IEEE Transactions on Pattern Analysis and Machine Intelligence*, vol. 6, no. 11, pp. 721–741, November 1984. 1

[3] A. K. Katsaggelos, *Digital Image Restoration*. Springer Publishing Company, Incorporated, 1991. 1

[4] S. Acton and A. Bovik, "Piecewise and local image models for regularized image restoration using cross-validation," *IEEE Trans on Image Processing*, vol. 8, no. 5, pp. 652–665, 1999. 1

[5] M. Haindl and J. Filip, *Visual Texture*, ser. Advances in Computer Vision and Pattern Recognition. London: Springer-Verlag London, January 2012. 1

[6] Y. Dong, A. Milne, and B. Forster, "A review of sar speckle filters: texture restoration and preservation," in *Geoscience and Remote Sensing Symposium, 2000. Proceedings. IGARSS 2000. IEEE 2000 International*, vol. 2, 2000, pp. 633–635 vol.2. 1

[7] H. Yamauchi, J. Haber, and H.-P. Seidel, "Image restoration using multiresolution texture synthesis and image inpainting," in *Computer Graphics International, 2003. Proceedings*, July 2003, pp. 120–125. 1

[8] V. Kolmogorov and C. Rother, "Minimizing nonsubmodular functions with graph cuts—a review," *Pattern Analysis and Machine Intelligence, IEEE Transactions on*, vol. 29, no. 7, pp. 1274–1279, 2007. 1

[9] T. Brox and D. Cremers, "Iterated nonlocal means for texture restoration," in *Scale Space and Variational Methods in Computer Vision*. Springer, 2007, pp. 13–24. 1

[10] E. A. Pneumatikakis and P. Maragos, "An inpainting system for automatic image structure-texture restoration with text removal," in *Image Processing, 2008. ICIP 2008. 15th IEEE International Conference on*. IEEE, 2008, pp. 2616–2619. 1

[11] C. Rother, P. Kohli, W. Feng, and J. Jia, "Minimizing sparse higher order energy functions of discrete variables," in *Computer Vision and Pattern Recognition, 2009. CVPR 2009. IEEE Conference on*. IEEE, 2009, pp. 1382–1389. 1

[12] t. Zhang, Q. Gao, and G. Tan, "Texture preserving image restoration with dyadic bounded mean oscillating constraints," *Signal Processing Letters, IEEE*, vol. 22, no. 3, pp. 322–326, March 2015. 1

[13] A. Dempster, N. Laird, and D. Rubin, "Maximum likelihood from incomplete data via the em algorithm," *Journal of the Royal Statistical Society, B*, vol. 39, no. 1, pp. 1–38, 1977. 2

[14] M. Haindl, "Visual data recognition and modeling based on local markovian models," in *Mathematical Methods for Signal and Image Analysis and Representation*, ser. Computational Imaging and Vision, L. Florack, R. Duits, G. Jongbloed, M.-C. Lieshout, and L. Davies, Eds. Springer London, 2012, vol. 41, ch. 14, pp. 241–259, 10.1007/978-1-4471-2353-8_14. [Online]. Available: http://dx.doi.org/10.1007/978-1-4471-2353-8_14 2, 3

[15] M. Haindl and S. Šimberová, "A scratch removal method," *Kybernetika*, vol. 34, no. 4, pp. 423–428, April 1998. 2, 3, 5

[16] M. Haindl and M. Kudělka, "Texture fidelity benchmark," in *Computational Intelligence for Multimedia Understanding (IWCIM), 2014 International Workshop on*. Los Alamitos: IEEE Computer Society CPS, November 2014, pp. 1 – 5. [Online]. Available: <http://ieeexplore.ieee.org/stamp/stamp.jsp?tp=&arnumber=7008812&isnumber=7008791> 2

[17] M. Haindl, "Recursive model-based colour image restoration," *Lecture Notes in Computer Science*, no. 2396, pp. 617–626, August 2002. 3

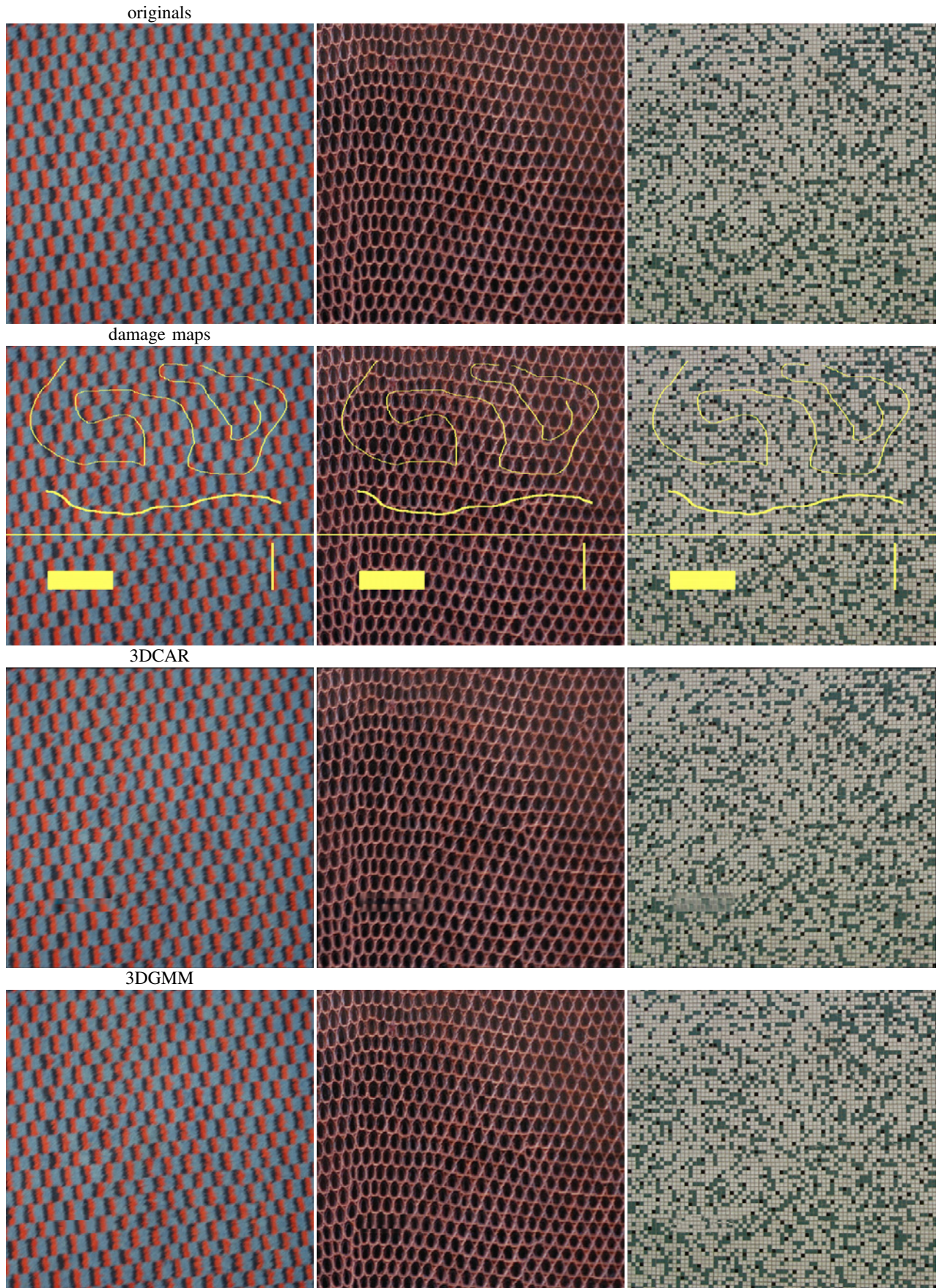


Fig. 3. Scratch restoration results for the carpet, cobra skin, and tiles textures.